

Stacked High-Impedance Surface (HIS) for 5 GHz WLAN Applications

Peter KOVÁCS, Jan PUSKELY

Dept. of Radio Electronics, Brno University of Technology, Purkyňova 118, 612 00 Brno, Czechia

kovacsp@feec.vutbr.cz, puskelj@feec.vutbr.cz

Abstract. *In this work we present a stacked high-impedance surface (HIS) for low-profile, high-gain, 5 GHz WLAN antennas. The structure consists of two layers: a lower mushroom layer and an upper planar layer. We demonstrate that the stacked geometry has much better properties than conventional single-layer structures for achieving simultaneously surface-wave suppression and zero reflection phase at a given frequency. We show by measurements that the designed stacked HIS exhibits both a large band gap and in-phase wave reflection over the entire range from 4.6 GHz to 6.4 GHz. The structure is realized on FR4 substrate using standard etching technology to make fabrication easy and cheap.*

Keywords

Antenna, high-impedance surface (HIS), in-phase wave reflection, surface-wave.

1. Introduction

High-impedance surfaces (HIS) are widely used in microwave and antenna engineering such as filters, substrates with suppressed surface-wave propagation or artificial magnetic conductors, i.e. surfaces that reflect the impinging electromagnetic waves in-phase. An electromagnetic structure having high surface impedance was introduced in 1999 by Sievenpiper and became known as the “mushroom” [1]. The geometry of the mushroom structure is analogous to a corrugated metal surface in which the corrugations have been folded up into lumped-circuit elements and distributed in a two-dimensional lattice. The height of such a structure is lower than a one-quarter wavelength and the distance between neighboring cells (periodicity) is much less than one wavelength [1].

In this paper we focus on the design of a high-impedance surface with both suppressed surface-wave propagation and in-phase wave reflection at 5.5 GHz. The main challenge is to cover the wireless local area network (WLAN) bands at this frequency using the commercially available and cheap dielectric FR4. The outcome of our research should be a cost-friendly, easy-to-fabricate high-

impedance surface for low-profile, high-gain WLAN antennas.

The major problem to overcome in the design of conventional mushroom structures realized on FR4 (relative permittivity $\epsilon = 4.15$ and height $h = 1.52$ mm) is to achieve zero reflection phase at 5.5 GHz and a surface-wave band-gap. The reason is that both the surface-wave band gap and the frequency of in-phase wave reflection crucially depend on parameters of the dielectric substrate and drift with variation of them [2], [3], [4]. We will show in practice that placing second, planar layer over the mushroom, the two different desirable properties can be tuned separately, almost independently of each other. This is due to the fact that the surface-wave suppression band is influenced with the parameters of both the lower mushroom and the upper planar layer, whereas the in-phase properties depend primarily on the parameters of the upper planar layer, especially on the size of the metallic patch, as discussed in [5]. In addition, the stacked geometry leads to a reduced size of the unit cell.

The idea of stacked high-impedance surface has been introduced by Sievenpiper [1]. He described the possibility of size reduction of unit cell by three-layer structures. Abhari and Eleftheriades presented a stacked structure for noise suppression in parallel-plate waveguides [6]. Feresidis et al. investigated the band-stop properties of double-layer dipole and tripole arrays [7]. However, to the best of our knowledge no researcher studied yet the effect of the second layer on the position of the surface-wave band gap in combination with the frequency of zero reflection phase.

This paper is organized by the following way. First, we design, for surface-wave band gap and zero reflection phase at 5.5 GHz, two HIS structures: a conventional single-layer mushroom one and one according to our dual-layer stacked principle. The simulated results for the two structures are compared, showing promise for our approach. Then, the optimized stacked structure is fabricated and measured. Also, we review the influence of the upper planar layer on features of the structure. Finally, we study the performance of a horizontal wire antenna placed on the high-impedance surface, demonstrating the fulfillment of the desired properties.

All computer simulations presented in the paper were done in CST Microwave Studio.

2. Design of HIS

The two high-impedance surfaces under investigation are shown in Fig. 1. The first is a conventional single-layer mushroom one and the second one is a dual-layer structure with mushroom unit cells at the bottom and planar square patches on the top. In comparison with other stacked high-impedance surfaces (e.g. presented in [8]) the one investigated in this work has the features of very simple construction and much larger bandwidth (over 30 %).

To design the structures, we used a particle swarm optimization (PSO) algorithm. We defined the objective function to consider both position of the band gap and its bandwidth and also frequency of the zero reflection phase. A detailed description of the algorithm we give in [5]. State variables for the structures are noted in Fig. 1: period D and size of square metallic patches P , P_2 were optimized with an accuracy of 0.1 mm; possible values of via diameter d were defined as 0.6 mm, 0.8 mm or 1.0 mm.

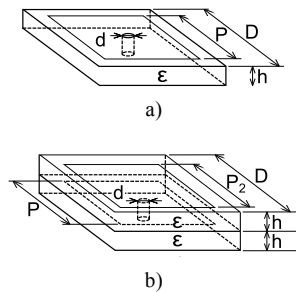


Fig. 1. High-impedance surfaces: mushroom (a), stacked (b).

Results of the design process are summarized in Tab. 1 (in this table, f_{CBG} is the central band gap frequency, BW is the relative bandwidth of the band gap and f_{ZRP} is the frequency of the zero reflection phase). It should be noted that in the case of the conventional mushroom HIS frequency of the zero reflection phase ($f_{ZRP} = 6.0$ GHz) is significantly shifted to the upper limit of the surface-wave band gap, whereas in the case of the stacked HIS, it lies exactly in the centre ($f_{ZRP} = 5.5$ GHz) of forbidden frequency band. This fact confirms that using the dual-layer geometry we are able to fulfill the prerequisites which are impossible to achieve for the single-layer mushroom structure.

	Mushroom	Stacked
D [mm]	8.3	7.3
P [mm]	7.9	6.1
P_2 [mm]	–	6.0
d [mm]	1.0	0.8
f_{CBG} [GHz]	5.41	5.47
BW [%]	36.4	32.5
f_{ZRP} [GHz]	5.96	5.51

Tab. 1. Optimization results for HIS.

3. Fabrication and Measurement

As mentioned above, the designed high-impedance surface with stacked geometry was realized on FR4 sub-

strate (pictures of the fabricated prototype are shown in Fig. 2). The dielectric slabs with mushroom and planar unit cells (18 x 18 cells each) were assembled and fixed with polyamide screws. It is important to notice that between the slabs a gap occurs which was not taken into account in the design. However, based on computer simulations, presence of a small gap does not critically influence neither the position of the band gap nor the frequency of the zero reflection phase.

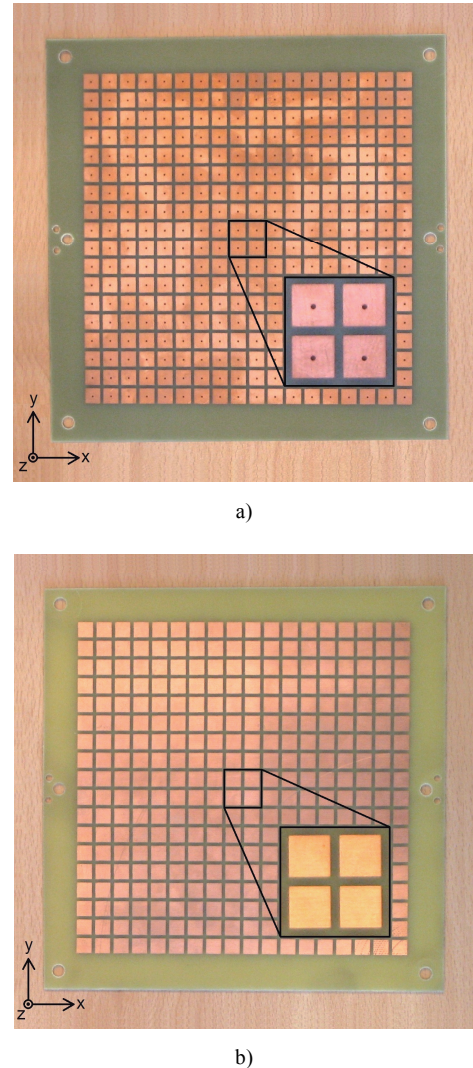


Fig. 2. The fabricated stacked high-impedance surface: the lower mushroom layer (a), the upper planar layer (b). Insets show details of the layers.

First, we measured the surface-wave properties of the fabricated prototype using two vertical coaxial probes placed on opposite sides of the board (corresponding to Γ -X direction in the dispersion diagram, where the band gap reaches its narrowest limits). The vertical probes make it possible to record the transmission for transverse magnetic (TM) waves. We realized two identical measurements: in the first step we investigated the TM surface-wave transmission on the fabricated HIS; in the second step we did the same using a conventional metal plate. The transmission characteristics of the HIS relative to the transmission

of the metal plate together with the calculated dispersion diagram are shown in Fig. 3(a) and Fig. 3(b). Measurements acknowledge computer simulations and reveal a strong transmission drop of over -10 dB in the frequency interval from 4.6 GHz up to 6.4 GHz. Next we explored reflection phase characteristics of the HIS for normal wave incidence, see Fig. 4. Frequency of the zero reflection phase $f_{ZRP} = 5.4$ GHz was measured. The frequency band within which the impinging electromagnetic wave is reflected in-phase rather than out-of-phase (i.e. absolute value of reflection phase is smaller than or equal to 90 deg) corresponds to the surface-wave band gap.

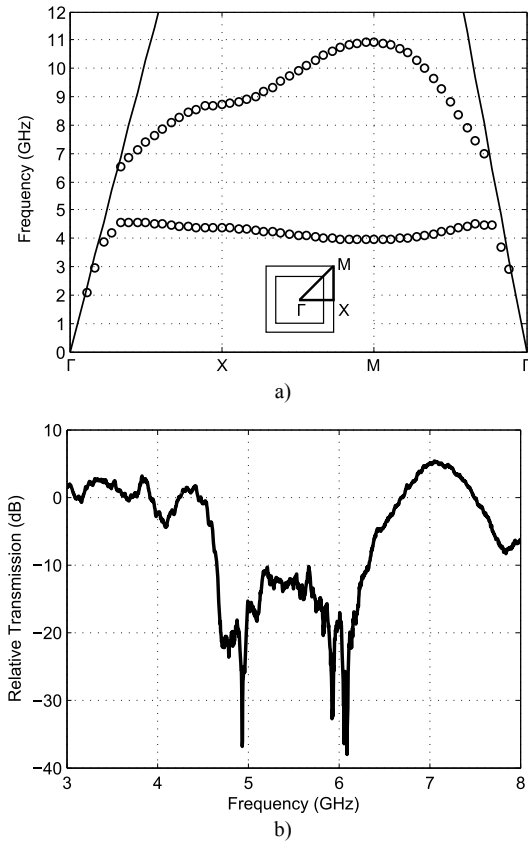


Fig. 3. Surface waves suppression over the stacked high-impedance surface: computer calculated dispersion diagram (a), measurement (b).

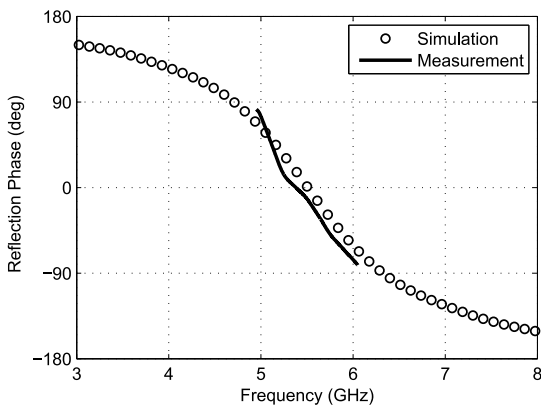


Fig. 4. Reflection phase diagram of the stacked high-impedance surface.

In order to find out the influence of the upper planar layer on properties of the stacked HIS, we repeated both surface-wave transmission and reflection phase measurements for the case with a removed upper layer. As shown in Fig. 5 and Fig. 6, the single mushroom structure exhibits a significantly narrower band gap with a central frequency of approximately 6.0 GHz and the frequency of the zero reflection phase is shifted to 8.8 GHz.

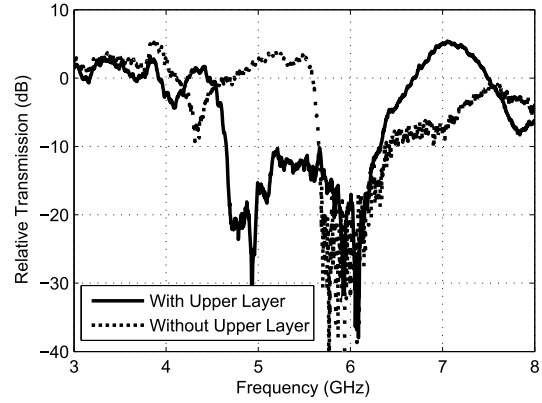


Fig. 5. Measured surface wave suppression over a stacked high-impedance surface with and without upper layer.

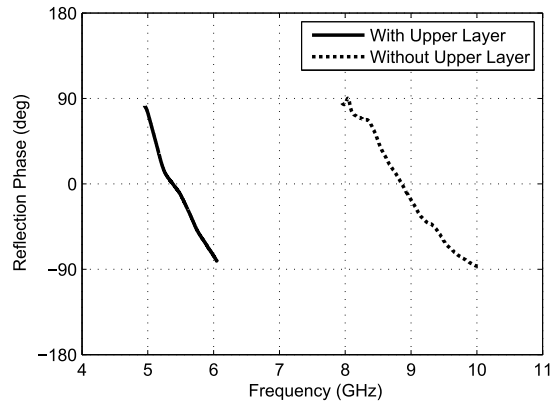


Fig. 6. Measured reflection phase diagram of the stacked high-impedance surface with and without upper layer.

4. Antenna Experiments

In this section we present measurement results of a horizontal wire antenna placed above the stacked high-impedance surface. The main goal is to demonstrate how the HIS influences radiation patterns of the antenna and to reduce the distance between the antenna and the reflector. We compare two cases: the antenna over the high-impedance surface and the antenna over a conventional metal ground plane. Impedance matching and radiation patterns were measured and antenna efficiency was calculated.

Fig. 7 shows a sketch of a wire antenna over stacked HIS. In this figure, l_a is the length of the antenna and h_a is the distance of the wire from the reflector. Due to strong interaction between the radiator and the surrounding medium, good impedance matching at the band gap central

frequency can only be achieved by separating the vertical part of the antenna from the HIS. This is possible by extending a feeding coaxial probe up to the upper layer of the structure.

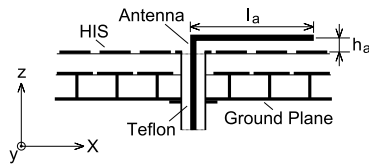


Fig. 7. Sketch of a horizontal wire antenna over stacked HIS.

In Fig. 8 the measured impedance matching of the wire antenna is depicted for three cases: a low-profile (LP) antenna over the HIS ($l_a = 41.0$ mm, $h_a = 2.5$ mm); a high-profile (HP) antenna over a simple metal ground plane ($l_a = 33.0$ mm, $h_a = 9.5$ mm); and a low profile antenna over a simple metal ground plane ($l_a = 41.0$ mm, $h_a = 2.5$ mm). The size of the reflector is the same for all three cases (160 mm x 160 mm). Apparently the antenna over the HIS indicates low reflection coefficient, even if the distance between the wire and the reflector is only $h_a = 2.5$ mm ($0.05 \lambda_0$ at 5.5 GHz). Similar result for the antenna over the metal ground plane was obtained for $h_a = 9.5$ mm ($0.17 \lambda_0$ at 5.5 GHz). Calculated antenna efficiency at 5.5 GHz is: 97 % (HIS – LP), 98 % (Metal – HP) and 10 % (Metal – LP); whereas the gain 4.8 dBi for HIS – LP and Metal – HP was obtained.

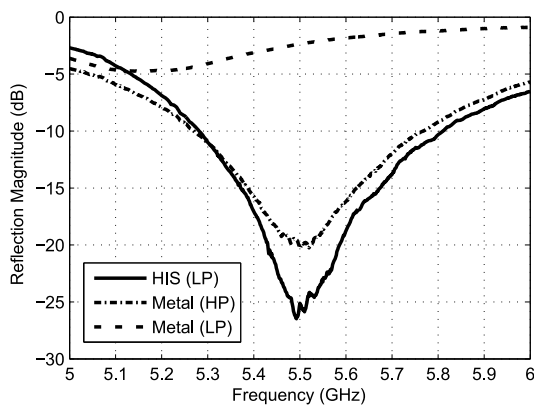


Fig. 8. Measured impedance matching of a horizontal wire antenna over stacked HIS and a conventional metal ground plane.

Measured radiation patterns of the horizontal wire antenna over the stacked HIS and metal ground plane are shown in Fig. 9. Suppression of surface-waves leads to significantly better front-to-back ratio and the radiated energy is focused into the upper hemisphere.

5. Conclusion

In this work we introduced a high-impedance surface for low-profile, high-gain, WLAN antennas. The main contribution of the paper is the use of a simple stacked geometry for the HIS in order to achieve simultaneous

surface-wave band gap and in-phase wave reflection at the required frequency 5.5 GHz using the FR4 substrate. We have shown that with the aid of an additive upper layer both band gap and reflection phase properties of a conventional mushroom structure can be significantly changed and tuned almost separately. Using similar structures, in cases when the single-layer mushroom one cannot meet the requirements, is straightforward.

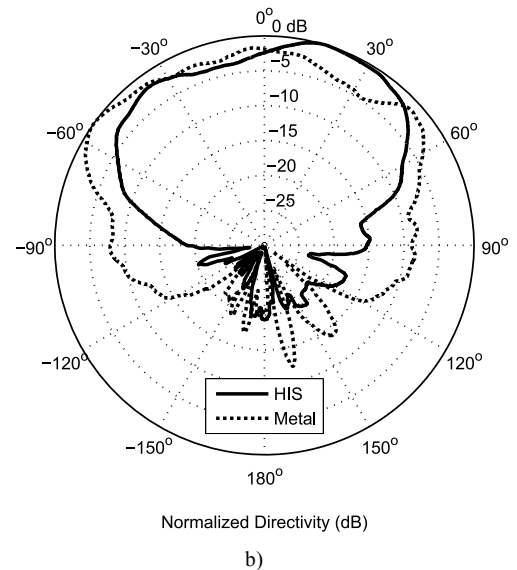
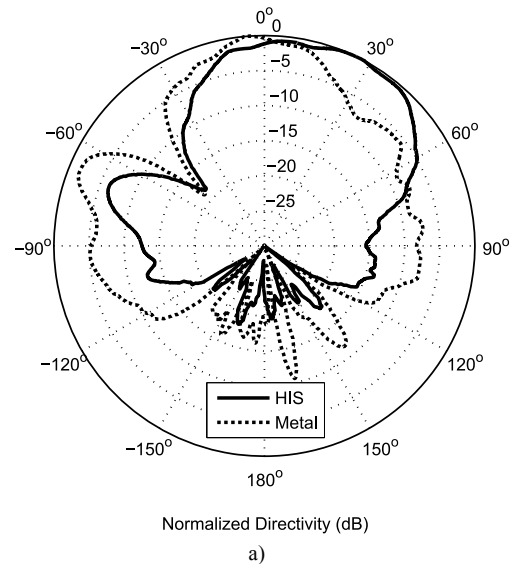


Fig. 9. Measured radiation patterns of the horizontal monopole antenna over the high-impedance surface and the conventional metal ground plane: xz- or E-plane (a), yz- or H-plane (b).

Acknowledgements

The research described in this paper was financially supported by the Czech Ministry of Education under grant no. LD12012. The support for project CZ.1.07/2.3.00/20.0007 WICOMT, financed from the operational program

Education for Competitiveness, is also gratefully acknowledged. Measurements were performed in laboratories supported by the SIX project; the registration number CZ.1.05/2.1.00/03.0072, the operational program Research and Development for Innovation.

The authors thank A. Vanžura and J. Voráč for fabricating the prototype and M. Zeman for measuring the antenna radiation patterns.

References

- [1] SIEVENPIPER, D. F., ZHANG, L., BROAS, R. F. J., ALEXOPOULOS, N. G., YABLONOVITCH, E. High-impedance electromagnetic surfaces with a forbidden frequency band. *IEEE Trans. Microw. Theory Tech.*, Nov. 1999, vol. 47, p. 2059 – 2074.
- [2] AMINIAN, A., YANG, F., RAHMAT-SAMIL, Y. In-phase reflection and EM wave suppression characteristics of electromagnetic bandgap ground planes. In *Proc. IEEE AP-S Int. Symp.*, June 22 – 27, 2003, vol. 4, p. 430 – 433.
- [3] CLAVIJO, S., DIAZ, R. E., MCKINZIE, W. E. Design methodology for Sievenpiper high-impedance surfaces: an artificial magnetic conductor for positive gain electrically small antennas. *IEEE Trans. Antennas Propag.*, Oct. 2003, vol. 51, p. 2678 – 2690.
- [4] LI, L., CHEN, Q., YUAN, Q., LIANG, C., SAWAYA, K. Surface-wave suppression bandgap and plane-wave reflection phase band of mushroomlike photonic bandgap structures. *J. Appl. Phys.*, Jan. 2008, vol. 103, no. 2, ID 023513.
- [5] KOVACS, P., RAIDA, Z., LUKES, Z. Design and optimization of periodic structures for simultaneous EBG and AMC operation. In

Proceedings of the 16th Conference on Microwave Techniques. Brno: Czechoslovakia Section IEEE, April 2010, p. 195-198.

- [6] ABHARI, R., ELEFThERIADES, G. V. Metallo-dielectric electromagnetic bandgap structures for suppression and isolation of the parallel-plate noise in high-speed circuits. *IEEE Trans. Microw. Theory Tech.*, June 2003, vol. 51, p. 1629 – 1639.
- [7] FERESIDIS, A. P., APOSTOLOPOULOS, G., SERFAS, N., VARDXOGLOU, J. C. Closely coupled metallodielectric electromagnetic band-gap structures formed by double-layer dipole and tripole arrays. *IEEE Trans. Antennas Propag.*, May 2004, vol. 52, p. 1149 – 1158.
- [8] BROAS, R. F. J., SIEVENPIPER, D. F., YABLONOVITCH, E. High-impedance ground plane applied to a cellphone handset geometry. *IEEE Trans. Microw. Theory Tech.*, July 2001, vol. 49, p. 1262 – 1265.

About Authors ...

Peter KOVÁCS was born in Slovakia. He received the Ph.D. degree from the Faculty of Electrical Engineering and Communication (FEEC), Brno University of Technology (BUT), Czech Republic, in 2011. Currently, he is with the Dept. of Radio Electronics FEEC BUT.

Jan PUSKELY was born in Přerov, the Czech Republic, in 1982. He received his master's degree in 2007 and his Ph.D. degree in 2011, both in Electrical Engineering from the Brno University of Technology. At present, he is with the Department of Radio Electronics, Brno University of Technology, as a researcher. His research interest is focused on measurements in the near field of antennas.